Scripta Materialia 214 (2022) 114673

Contents lists available at ScienceDirect

Scripta Materialia

journal homepage: www.journals.elsevier.com/scripta-materialia

Sluggish dynamics of homogeneous flow in high-entropy metallic glasses

L.T. Zhang [a], Y.J. Wang [b,c], E. Pineda [d], H. Kato [e], Y. Yang [f,g], J.C. Qiao [a,h,*]

[a] School of Mechanics, Civil Engineering and Architecture, Northwestern Polytechnical University, Xi'an 710072, China
[b] State Key Laboratory of Nonlinear Mechanics, Institute of Mechanics, Chinese Academy of Sciences, Beijing 100190, China
[c] School of Engineering Science, University of Chinese Academy of Sciences, Beijing 100049, China
[d] Department of Physics, Institute of Energy Technologies, Universitat Politècnica de Catalunya, 08019 Barcelona, Spain
[e] Institute for Materials Research, Tohoku University, Sendai 980-8577, Japan
[f] Department of Mechanical Engineering, College of Engineering, City University of Hong Kong, Tat Chee Avenue, Kowloon Tong, Kowloon, Hong Kong SAR, China
[g] Department of Materials Science and Engineering, College of Engineering, City University of Hong Kong, Tat Chee Avenue, Kowloon Tong, Kowloon, Hong Kong SAR, China
[h] Innovation Center, NPU-Chongqing, Chongqing 401135, China

ARTICLE INFO

Keywords:
High-entropy metallic glass
Mechanical relaxation
Creep
Free volume

ABSTRACT

A comparative study of high-entropy metallic glasses and their reference counterparts was conducted via mechanical relaxation behavior and high-temperature deformation. We show that the high-entropy metallic glasses possess a relatively more homogeneous structure, which generates smaller activation volumes and sluggish free volume evolution during high-temperature deformation. A spectrum analysis that allows to delineate the deformation details of high-entropy metallic glasses were constructed. The core finding sheds important light on the structural heterogeneity and sluggish dynamics and provides an essential piece for understanding the deformation mechanism of high-entropy metallic glasses.

Owing to the unique mechanical/physical properties, the metallic glasses (MGs) have attracted tremendous research interest in the field of materials science and condensed matter physics [1–3]. Traditionally, they have been prepared and rapidly developed according to a 'base element' paradigm. This strategy begins with one or two principal elements, such as Pd-based and Zr-based [4,5]. A novel theme of "more is different" for alloy design was postulated about two decades ago, this strategy involves the mixing of five or more principal elements in equimolar, or near equimolar, ratios (5~35 at.%) to form thermodynamically metastable alloys termed as high-entropy alloys (HEAs) [6,7]. The concept of HEAs boldly advances the design philosophy of alloys and offers the promise to discover interesting novel MGs with useful properties. Overlapping the characteristics of HEAs and MGs, high-entropy metallic glasses (HE-MGs) have been reported to present plenteous improved physical and mechanical properties [8,9]. The four core features of HEAs, i.e., high entropy, severe lattice distortion, sluggish diffusion and cocktail effects, have received the favor of the researchers [6,7]. After the extensive studies, an interesting question has been raised: how does the entropy-induced sluggish diffusion effect exist and to what extent it governs the structure-property relation of HE-MGs? Nevertheless, given the short history of research on HE-MGs, the field is still in fumbling stage compared to that of the conventional MGs.

At ambient temperature, most of the MGs exhibit poor tensile plasticity which represents an "Achilles' heel" of the generic glassy materials [10,11]. In sharp contrast, MGs actually show homogeneous flow and pronounced plasticity at $T \geq 0.8\ T_g$ (T_g is the glass transition temperature), paving the way to study the details by which the constituent atoms rearrange themselves individually and cooperatively under thermal/-mechanical stimulations [12,13]. Besides, the deformation mechanism of MGs has been found to be closely bound to the relaxation behaviors [14,15]. There are two main processes governing the relaxation of MGs: the initial fast process (β relaxation) viewed as locally reversible rearrangement and the final slow process (α relaxation) associated with the large scale irreversible rearrangement of atoms [16,17].

The purpose of the current work is to give a picture on the homogeneous flow behavior in an attempt to gain further insight into the physical metrics of the sluggish dynamics observed in HE-MGs. Compared with the reference MGs, a smaller activation volume and slower annihilation of free volume are uncovered in the HE-MGs with different types of β relaxation behaviors, thus linking such properties to the higher mixing entropy. More significantly, we proposed a spectrum analysis to delineate the deformation mechanism governed by soft

* Corresponding author.
E-mail address: qjczy@nwpu.edu.cn (J.C. Qiao).

https://doi.org/10.1016/j.scriptamat.2022.114673
Received 19 December 2021; Received in revised form 8 March 2022; Accepted 9 March 2022
Available online 14 March 2022

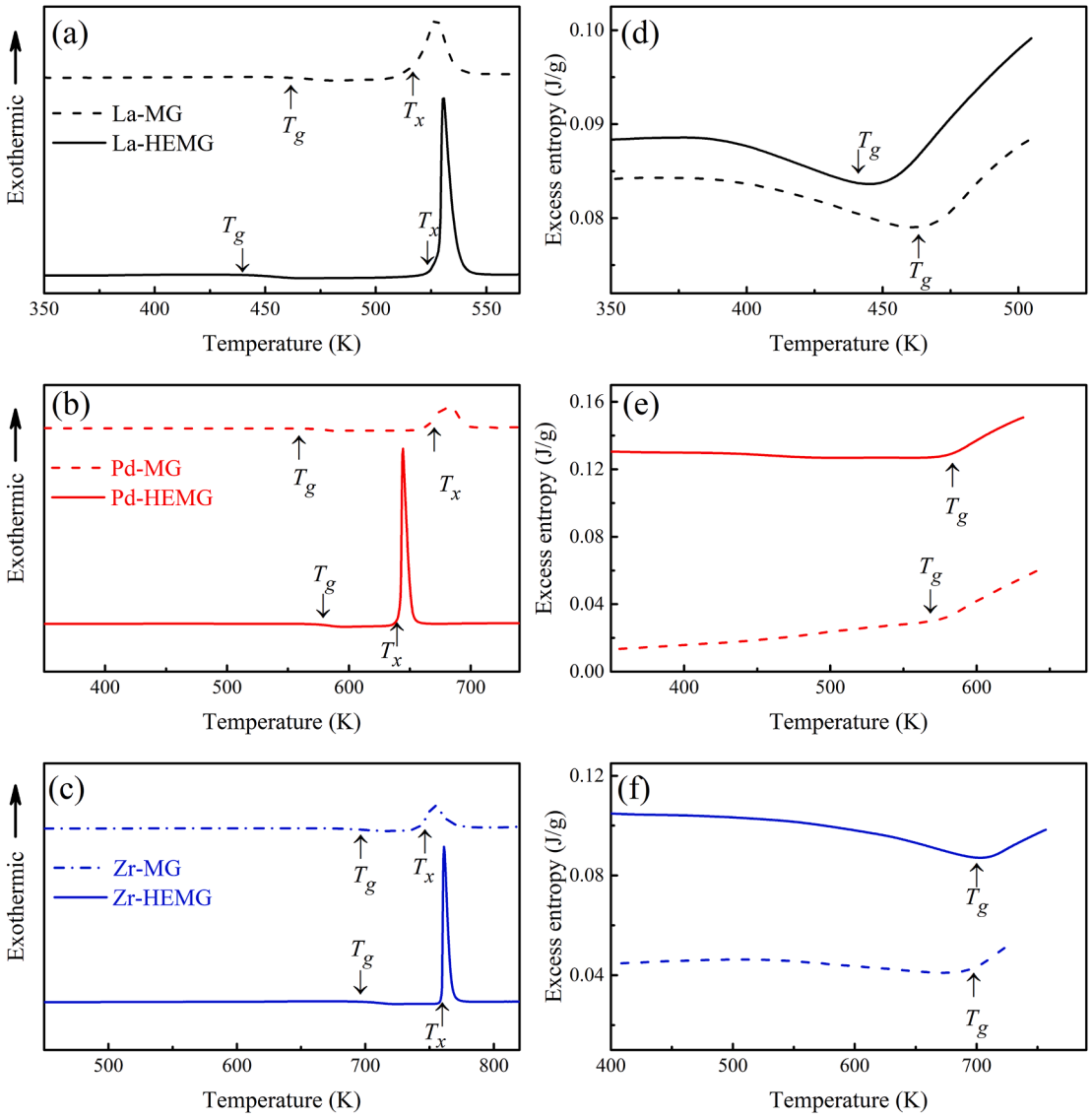

Fig. 1. (a)-(c) DSC curves for HE-MGs and their reference counterparts; (b)-(e) Evolution of the excess entropy on temperature for HE-MGs and their reference counterparts.

regions in HE-MGs.

$La_{60}Ni_{15}Al_{25}$ (at.%), $La_{30}Ce_{30}Ni_{10}Al_{20}Co_{10}$ (at.%), $Pd_{40}Cu_{30}Ni_{10}P_{20}$ (at.%), $Pd_{20}Pt_{20}Cu_{20}Ni_{20}P_{20}$ (at.%), $Zr_{45}Cu_{50}Al_5$ (at.%) and $Ti_{16.7}Zr_{16.7}Hf_{16.7}Cu_{16.7}Ni_{16.7}Be_{16.7}$ (at%) MGs were chosen as model alloys and fabricated by single-roller melt-spinning in an argon atmosphere into thin ribbons (thickness around 30 μm). Thermal analysis was carried out by differential scanning calorimeter (DSC, Netzsch DSC 404 F3) under high-purity argon flow. Characteristic temperatures like the glass transition temperature T_g and the crystallization temperature T_x were obtained from the corresponding DSC curves at a heating rate of 20 K/min. The absolute values of the specific heat capacity Δc_p of glasses (i.e., the difference between amorphous state between crystalline state) can be calculated by c_{p_glass}-$c_{p\_crystal}$.

The storage and loss moduli of the model glassy ribbons were measured by a commercial dynamic mechanical analysis (DMA, TA instruments Q800) using the tension film configuration. Under a simulation of sinusoidal stress $\sigma = \sigma_0\cos(2\pi ft)$, the strain response of typical viscous-elastic material can be monitored as $\varepsilon = \varepsilon_0\cos(2\pi ft + \delta)$, where f is the loading frequency and δ the phase lag. The complex Young's modulus can be expressed as $E = \sigma/\varepsilon = E' + iE''$ in the complex plane, where E' and E'' are the storage and loss moduli, respectively. The mechanical relaxation spectrums were determined at testing frequency of 2 Hz and heating rate of 2 K/min.

The tensile stress jump tests of the model glassy ribbons were performed in DMA in tensile mode at various normalized temperature from 0.80 T_g to 0.86 T_g. The applied stress was from 50 MPa to 225 MPa for La- and Pd-based MGs and from 100 MPa to 275 MPa for Zr-based MGs. The stress interval between the two segments was 25 MPa and the stress rate was 6.25 MPa/s. The loading time was 180 min for the first stress level and 30 min for the subsequent levels.

Fig. 1**(a)-(c)** show the Δc_p curves of HE-MGs and their reference counterparts. The glass transition temperature T_g and the onset temperature of crystallization T_x, are indicated. It starts with an endothermic heat effect due to the glass transition followed by an exothermic peak corresponding to the crystallization. Combining the measured specific heat capacity data and entropy of crystallization ΔS_{cry}, we can calculate the excess entropy of our systems as a function of temperature as $\Delta S(T) = \Delta S_{cry} - \int_T^{T_{equal}} \frac{\Delta c_p(T^*)}{T^*} dT^*$. T_{equal} is the temperature where the Gibbs free energy of the glass and the crystal are equal. After crystallization, the value of Δc_p is approximately equal to zero. For the

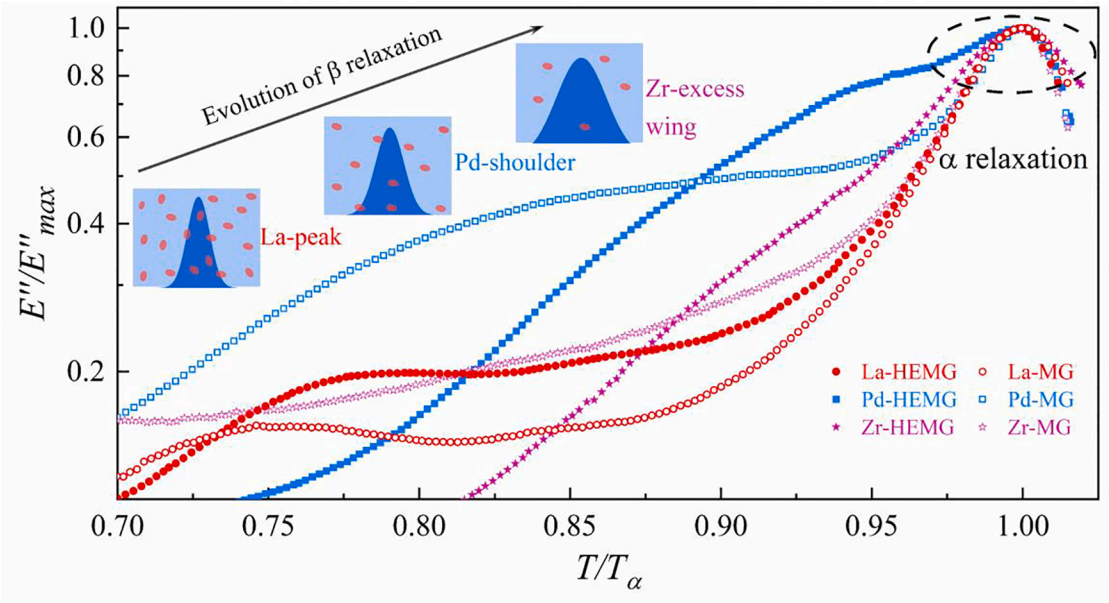

Fig. 2. Evolution of the normalized loss modulus E''/E''_{max} versus the normalized temperature T/T_α at a testing frequency of 2 Hz and heating rate of 2 K/min for $La_{30}Ce_{30}Ni_{10}Co_{10}Al_{20}$ HE-MG, $La_{60}Ni_{15}Al_{25}$ MG, $Pd_{20}Pt_{20}Cu_{20}Ni_{20}P_{20}$ HE-MG, $Pd_{40}Ni_{10}Cu_{30}P_{20}$ MG, $Ti_{16.7}Zr_{16.7}Hf_{16.7}Cu_{16.7}Ni_{16.7}Be_{16.7}$ HE-MG, and $Zr_{45}Cu_{50}Al_5$ MG respectively. E''_{max} is the maximum of loss modulus and T_α is the peak temperature of the main α relaxation. The inset gives the schematic illustration of the relationship between the density and distribution of soft regions and β relaxation behavior in MGs.

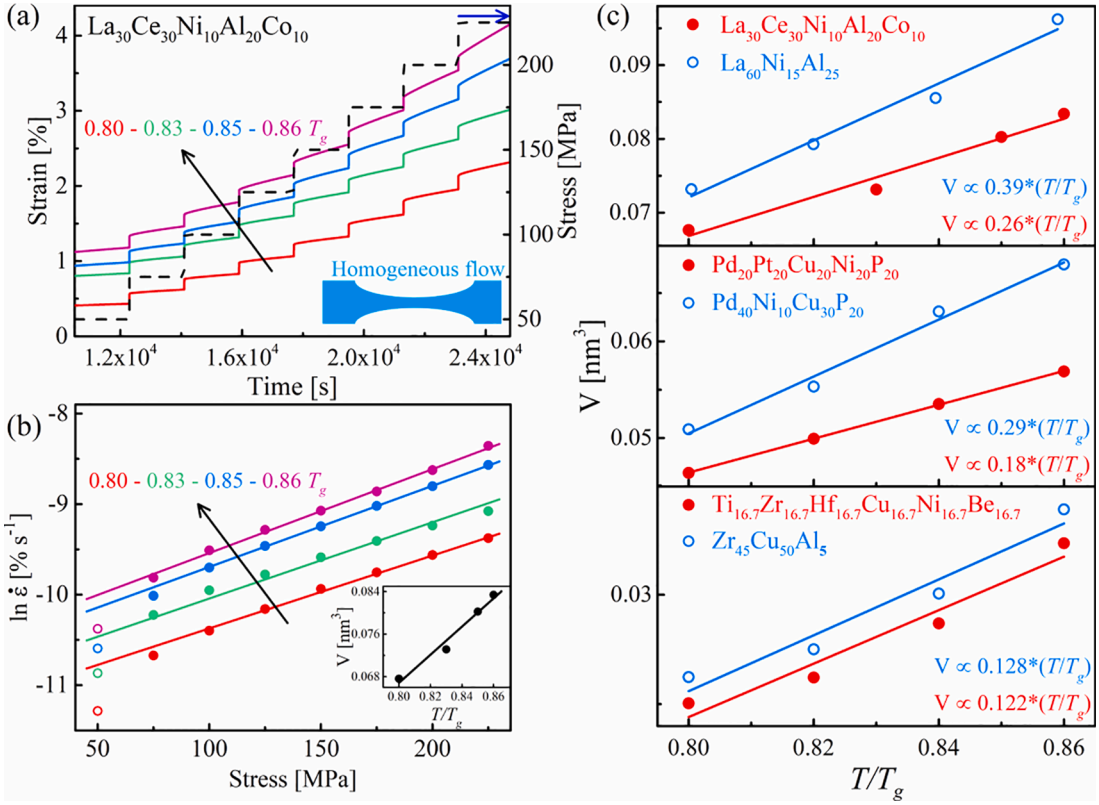

Fig. 3. (a) The stress-jump tests of $La_{30}Ce_{30}Ni_{10}Co_{10}Al_{20}$ HE-MG at 0.80, 0.83, 0.85, and 0.86 T_g. (b) Evolution of the strain rate on the applied stress at various temperature. The solid lines denote the linear fittings. Inset shows a quasi-linear relation between activation volume and temperature. (c) Variation of activation volume with T/T_g for $La_{30}Ce_{30}Ni_{10}Co_{10}Al_{20}$ HE-MG, $La_{60}Ni_{15}Al_{25}$ MG, $Pd_{20}Pt_{20}Cu_{20}Ni_{20}P_{20}$ HE-MG, $Pd_{40}Ni_{10}Cu_{30}P_{20}$ MG, $Ti_{16.7}Zr_{16.7}Hf_{16.7}Cu_{16.7}Ni_{16.7}Be_{16.7}$ HE-MG, and $Zr_{45}Cu_{50}Al_5$ MG respectively. The solid lines are linear fittings.

calculations we choose the end temperature of crystallization as T_{equal}. Figs. 1**(d)-(f)** show the evolution of excess entropy of HE-MGs and their reference counterparts on temperature. Obviously, HE-MGs possess a higher value of excess entropy than that of their reference counterparts. The measurement of Δc_p plays an essential role in quantificationally describing the excess entropy of HE-MGs.

Fig. 2 shows the evolution of the normalized loss modulus E''/E''_{max} on the normalized temperature T/T_α at a testing frequency of 2 Hz and heating rate of 2 K/min., There exists an additional peak at low temperature besides the main α relaxation in the E''/E''_{max} curve of La-based MGs, which is clearly discerned as β relaxation. For Pd-based MGs the β relaxation is a type of "shoulder", while it is the α relaxation that dominates the E''/E''_{max} curve of Zr-based MGs. Only an excess wing at the low temperature side of the α relaxation peak is observed in these latter systems. Therefore, in this work we selected a set of compositions with a quite different manifestation of the β relaxation.

MGs are highly structurally heterogeneous and can be modeled as soft regions confined by the surrounding elastic matrix [18,19]. Some researchers have proposed that the atoms in soft regions possess lower elastic modulus and packing density but higher mobility, which can be easily activated and rearranged in a local environment of stress or temperature [20]. Furthermore, the β relaxation has been recently associated to the motion of string-like of loosely packed atoms in these soft regions, which is rooted in the structural heterogeneity inherited from their liquid states [21,22]. The β relaxation behaviors are quite different in various MGs attributed to the totally different densities, intrinsic relaxation times, and energy distributions of the soft regions (as seen in the inset of Fig. 2) [23].

Stress jump tests were applied at a wide range of stress and temperature. Fig. 3**(a)** illustrates the strain evolution of flow processes occurring in La-based HE-MG at different normalized temperatures (scaled by T_g for comparison). Only the results of La-based HE-MG are shown in the main text and the others are shown in ***SI Appendix, Fig. S1***. The experimental results show that the strain and strain rate increase with the increase of the stress or temperature, indicating a larger volume fraction of atoms in the matrix is activated and transforms into soft regions. The deformation units in MGs carrying the plastic deformation are activated by thermal and mechanical stimulations, and the strain rate can be described as [13]

$$\dot{\varepsilon} = \dot{\varepsilon}_0 \exp\left(-\frac{\Delta H}{k_B T}\right) = \dot{\varepsilon}_0 \exp\left(-\frac{\Delta E - \tau V}{k_B T}\right) \tag{1}$$

where $\dot{\varepsilon}_0$ is a strain rate pre-factor, k_B is the Boltzmann constant, ΔH is the activation free enthalpy for the stress-assisted, thermally activated plastic deformation, ΔE is the activation energy of the plastic deformation unit, and V is the activation volume. The activation enthalpy is $\Delta H = \Delta E - \sigma V$, which levels the role of mechanical work in biasing the potential energy landscape. Considering the plastic deformation in MGs is dominated by shear stress, we use an empirical relation $\tau = \sigma/\sqrt{3}$. The activation volume can be computed by the general partial differential of Eq. (1) as: $V = \sqrt{3} k_B T \frac{\partial \ln(\dot{\varepsilon})}{\partial \sigma}$. Fig. 3**(b)** shows the log of strain rate versus the stress at various temperatures, the solid lines were linear fittings. Here we gave the fitting results of the La-based HE-MG. Closer inspection reveals a systematic deviation of the experimental data from the fitted curve: the first data point (open symbols) shows slightly smaller strain rates than the values fitted. The reasons of such deviation may include two aspects: (i) The dynamic balance between the creation and annihilation of structural defects is not reached for quasi-steady-state creep because of the effect of net structural relaxation. (ii) The isothermal time is 180 min for the stress level of 50 MPa but only for 30 min for the subsequent levels. The continuous structural relaxation has a positive effect on decreasing the strain rate. We find that the activation volume quasi-linearly increases with the temperature in the region from 0.8~0.86 T_g [see the inset in Fig. 3**(b)**]. Furthermore, the activation volume of the six systems can be evaluated as shown in Fig. 3**(c)**. From the results, the following observation can be made:

(i) The activation volume quasi-linearly increases with increasing temperature, independently of the chemical compositions, pointing that the quasi-linear relation between activation volume and temperature is a universal characteristic of MGs;

(ii) MGs that possess a weaker β relaxation are relatively homogeneous and contain less soft regions [24]. The activation volume progressively increase as the β relaxation transforms from an "excess wing" to a "peak", proving that more heterogeneous structure facilitates larger activation volume;

(iii) The slope stands for the increase rate of the activation volume. The comparison between HE-MGs and their reference counterparts shows the former with smaller slope, which indicates the former may possess a relatively homogeneous structure;

(iv) The difference of the value and increase rate of activation volume between HE-MGs and their reference counterparts strongly depends on the β relaxation mode. Such a significant difference exists between La-based MGs but is almost negligible between Zr-based MGs. It indicates that the higher the density of soft regions, i.e., the more heterogeneous the structure, the more affected by the high entropy effect.

Johnson and Samwer proposed a cooperative shearing model (CSM) to elucidate the plasticity of MGs below the T_g [25]. In the framework of CSM, the stress-assisted activation enthalpy, ΔH at finite stress $0<\tau<\tau_c$ is expressed as $\Delta H = 4R_0 G\gamma_c^2\left(1-\frac{\tau}{\tau_c}\right)^{\frac{3}{2}}\xi\Omega$, where G is the shear modulus, τ_c is a threshold shear resistance at zero temperature, Ω is the volume of the shear transformation zones, and $\gamma_c \approx 0.027$, $R_0 \approx 0.25$, and $\xi \approx 3$ are constants [25]. From the tension stress jump tests, one can compute the shear transformation zones volume as $\Omega = \frac{V\tau_c}{6R_0 G\gamma_c^2 \xi\left(1-\frac{\tau}{\tau_c}\right)^{\frac{1}{2}}}$. The average atomic radius R_a is statistically computed by $R_a = \sum_{j=1}^{n} x_j r_j^3$, where x_j is the mole fraction of the jth element, r_j is the atomic radius of the jth element. Therefore, the number of atoms during plastic deformation in MGs can be evaluated, as summarized in ***SI Appendix, Table 1*** for details. According to our fittings, it is reasonably expected that the number of atoms varies from 7.0 to 16.7 in the supercooled liquid region, which is closely near to the number reported for other MGs, verifying the homogeneous flow of MGs obeys a similar mode [26].

Structural relaxation results in a progressive increase of the structural ordering and a decrease of atomic mobility [27]. Note that the plastic deformation of MGs occurs by the superposition of the shear of multiple localized groups of atoms, and it also has a rejuvenation effect creating soft regions [28,29]. As a consequence, the population of soft regions decreased by structural relaxation and increased by plastic deformation, the latter mitigating the effect of structural relaxation or even equilibrating it in case of a sufficient power density (the product of the stress and strain rate). The plastic deformation of MGs is actually accompanied by shear dilatation [30], thus, there is a competition between the annihilation of free volume induced by the structural relaxation and the creation introduced by plastic deformation. The relation between free volume and the structural defects concentration c_f is defined as $c_f = \exp\left(-\frac{\mu\nu_c}{\nu_f}\right)$, where μ is a pre-factor between 0.5 and 1, ν_c is the critical value of free volume and ν_f is the average free volume per atom [31]. Taking annihilation and creation of free volume into account, the expression of c_f is expressed as follows [31]:

$$\begin{cases} \dot{c}_f + -k_r c_f\left(c_f - c_{f,eq}\right) + a_x \dot{\varepsilon} c_f \ln^2\left(c_f\right) \\ \dot{\varepsilon} = \dot{\varepsilon}_f \sinh\left(\frac{\sigma\varepsilon_0 v_0}{2\sqrt{3}k_B T}\right) + \left(\frac{\dot{\sigma}}{E}\right) \end{cases} \tag{2}$$

where k_r is the rate constant, $c_{f,eq}$ is the equilibrium flow defect concentration at a finite temperature, a_x is the proportionality factor, n is the number of activated atoms, and E is the elastic modulus. In the steady-state flow region, c_f reaches a stationary value and then a balance between the annihilation and the creation of free volume is established. The evolution of the strain and flow defect concentration during the

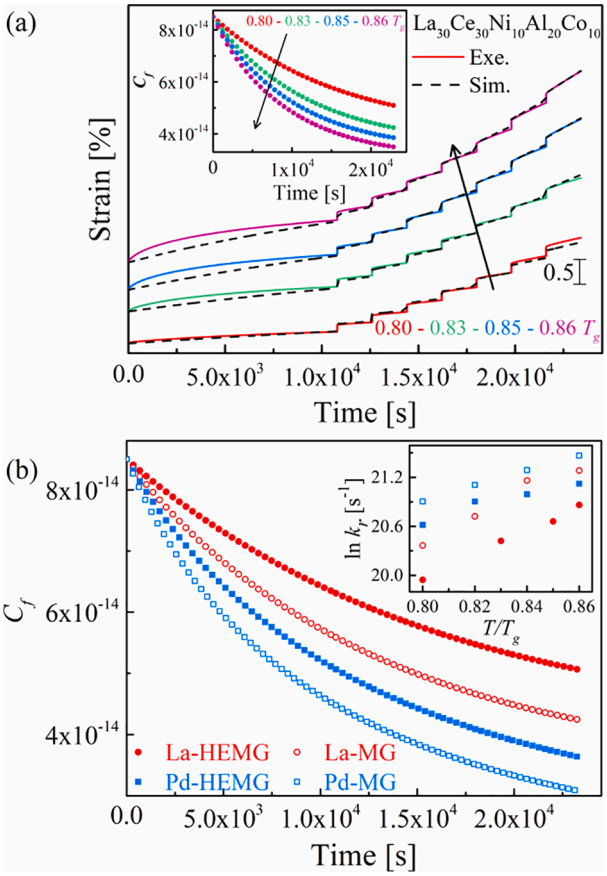

Fig. 4. (a) The simulated results of the strain-time curves for $La_{30}Ce_{30}Ni_{10}Co_{10}Al_{20}$ HE-MG at various temperatures. Inset shows the evolution of the flow defect concentration with time at various temperatures. (b) Evolution of the flow defect concentration with time for La-based and Pd-based MGs and HE-MGs. Inset shows evolution of the k_r on the normalized temperature T/T_g. .

tension stress jump tests was calculated by numerical integration of Eq. (2). The initial flow defect concentration c_0 was estimated at 8.5×10^{-14} for all of systems to remove the influence of numerical fault. The final value of c_f for each test was taken as the input value for the next test. The free parameters, k_r and a_x, were adjusted to fit the complete set of data points.

According to free volume theory, the stress-strain curves were simulated by Eq. (2), as shown in Fig. 4**(a)**. We show the simulation of the La-based HE-MG in the main text and the others in ***SI Appendix, Fig. S2***. The deviation may be induced by the influence of $\varepsilon_0\nu_0$,E, and ribbon size. The variation of ribbon size during tension (details seen in the inset of Fig. 3**(a)**) leads to an inaccurate true stress and elastic modulus, which have further influence on the flow defects concentration. The inset of Fig. 4**(a)** depicts the evolution of corresponding defects concentration during the stress jump tests for La-based HE-MG. The increase of the temperature accelerates the annihilation of flow defect concentration (aging) while the increase of the applied stress can accelerate the creation of flow defect concentration (rejuvenation). Only when a stress beyond the threshold is applied, such a thermo-mechanical creep can induce the structural disordering [32].

To shed some light on the mechanism responsible for the observed occurrence of smaller activation volume and increase rate in HE-MGs, we compared the defects evolution as a function of the time for La-based and Pd-based HE-MGs and their reference counterparts (Fig. 4 **(b)**). One can see that the curve of HE-MGs is obviously lower than that of their reference counterparts, confirming a slower free volume annihilation rate and sluggish dynamics. The k_r values obtained from the fits are shown in the inset in Fig. 4**(b)** as a function of T/T_g for better comparison. At first sight, it seems plausible that the unexpected sluggish dynamics can be ascribed to a smaller annihilation rate coefficient.

The plastic deformation of MGs is considered to activate the soft regions, facilitating to reach the percolation of active flow zones. The correlation between the deformation and atomic cooperative rearrangements has been also reported in polymeric and silica glasses, where the segmental mobility of polymer chains significantly increases during the tensile creep [33], and the atomic-scale localized rearrangements have even been directly observed by the transmission electron microscope [34]. The way of sluggish dynamics to simulate such a relationship

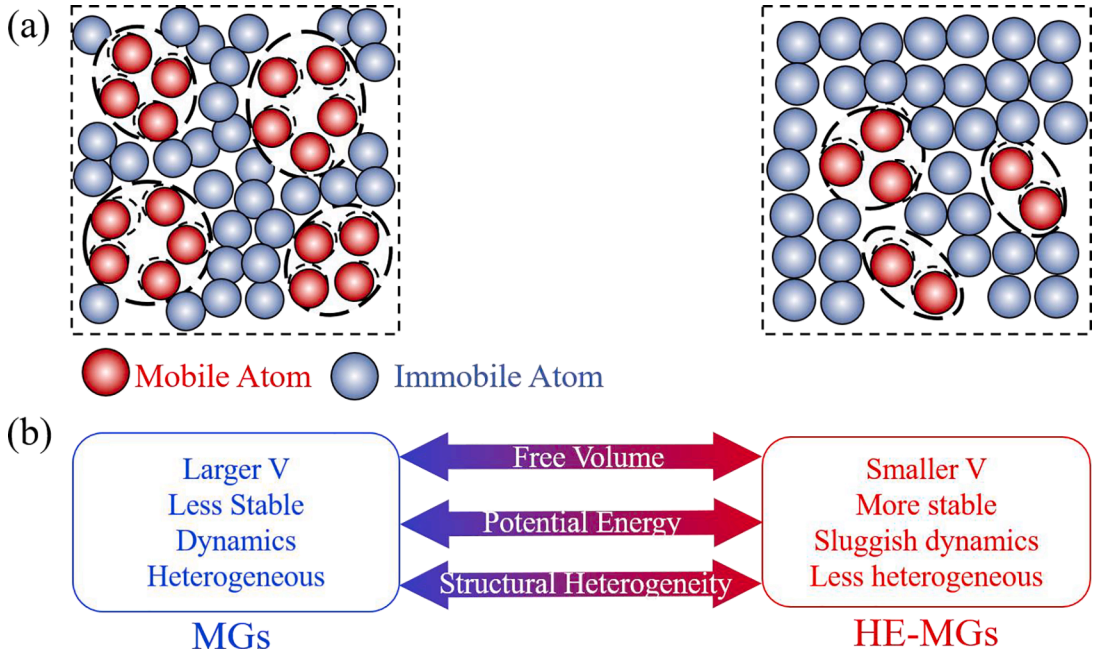

Fig. 5. (a) Schematic diagram of microstructure and activation volumes in HE-MGs and their counterparts. HE-MGs present relatively homogeneous microstructure which might be induced by the high entropy; (b) The structural indicators of HE-MGs and their counterparts. The various keywords are used to qualitatively describe the structural states.

deserves additional studies. The potential energy landscape (PEL) has been widely applied into investigating the physical phenomena of MGs such as the glass transition [35], physical aging [36], and mechanical deformation [14]. Obtained by rapid freezing from the melt, the energy level of MGs is relatively higher than that of their crystalline counterparts and the state locates at a high-energy basin [23,37]. During an isothermal annealing, MGs progressively trigger the annihilation of free volume and fall into a low-energy basin. Due to lower Gibbs free energy, HE-MGs are most likely located at a relatively low-energy basin compared with that of their reference MGs. Akin to previous results, HE-MGs possess excellent high-temperature stability in the supercooled liquid region, suggesting a higher activation energy for crystallization [38,39]. **Fig. 5(a)** is a schematic diagram of microstructure and activation volumes in HE-MGs and their counterparts. From the results shown in this work, HE-MGs with relatively homogeneous structures inhibit the atomic rearrangements, thus, possessing relatively small activation volume. Similar sluggish dynamics in HE-MGs have been also recently observed in various glasses [39–41]. In addition, we also illustrate the correlations between HE-MGs and their counterparts, as well as the structural state they correspond to (**Fig. 5(b)**). Our findings validate the existence of the entropy-induced sluggish dynamics in HE-MGs: the high entropy strategy to design new compositions generates glass structures restraining the atomic rearrangements. These processes are found to be coupled through soft regions that characterize the sluggish dynamics of the system.

In conclusion, we explored the sluggish dynamics in HE-MGs via mechanical relaxation and high-temperature deformation, which will rise the interest in HE-MGs and will be useful for tailoring the mechanical deformation behavior of metallic glasses. High entropy introduces a small value and a weaker temperature dependence of the activation volume, as well as a smaller free volume annihilation coefficient, leading to sluggish dynamics. These findings extend our knowledge of HE-MGs and provide a significant piece of new information to sketch a more complete structure-property relation of these materials.

Declaration of Competing Interest

The authors declare that they have no known competing financial interests or personal relationships that could have appeared to influence the work reported in this paper.

Acknowledgments

This work is supported by the NSFC (Grant No. 51971178), the Natural Science Basic Research Plan for Distinguished Young Scholars in Shaanxi Province (Grant No. 2021JC-12) and the Natural Science Foundation of Chongqing (Grant No. cstc2020jcyj-jqX0001). The investigation of L.T. Zhang is sponsored by Innovation Foundation for Doctor Dissertation of Northwestern Polytechnical University (Grant No. CX2021015). YJW was financially supported by NSFC (Grant No. 12072344) and the Youth Innovation Promotion Association of the Chinese Academy of Sciences. E. Pineda acknowledges financial support from 'Proyecto PID2020–112975GB-I00 de investigación financiado por MCIN/AEI /10.13039/501100011033' and Generalitat de Catalunya AGAUR grant 2017-SGR-42. The research of YY is supported by the Research Grants Council, the Hong Kong government, through the General Research Fund (GRF) with the grant numbers CityU11200719 and CityU11213118.

Supplementary materials

Supplementary material associated with this article can be found, in the online version, at doi:10.1016/j.scriptamat.2022.114673.

References

[1] J.C. Qiao, Q. Wang, J.M. Pelletier, H. Kato, R. Casalini, D. Crespo, E. Pineda, Y. Yao, Y. Yang, Prog. Mater. Sci. 104 (2019) 250–329.
[2] W.L. Johnson, Prog. Mater. Sci. 30 (2) (1986) 81–134.
[3] W.H. Wang, Prog. Mater. Sci. 106 (2019), 100561.
[4] H.S. Chen, D. Turnbull, Acta Metall. 17 (8) (1969) 1021–1031.
[5] A. Peker, W.L. Johnson, Appl. Phys. Lett. 63 (17) (1993) 2342–2344.
[6] E.P. George, D. Raabe, R.O. Ritchie, Nat. Rev. Mater. 4 (8) (2019) 515–534.
[7] J.W. Yeh, S.K. Chen, S.J. Lin, J.Y. Gan, T.S. Chin, T.T. Shun, C.H. Tsau, S.Y. Chang, Adv. Eng. Mater. 6 (5) (2004) 299–303.
[8] M. Yang, X. Liu, Y. Wu, H. Wang, X. Wang, Z. Lu, Mater. Res. Lett. 6 (9) (2018) 495–500.
[9] A. Takeuchi, N. Chen, T. Wada, Y. Yokoyama, H. Kato, A. Inoue, J.W. Yeh, Intermetallics 19 (10) (2011) 1546–1554.
[10] Z.F. Zhang, G. He, J. Eckert, L. Schultz, Phys. Rev. Lett. 91 (4) (2003), 045505.
[11] A. Inoue, B. Shen, H. Koshiba, H. Kato, A.R. Yavari, Nat. Mater. 2 (10) (2003) 661–663.
[12] J. Lu, G. Ravichandran, W.L. Johnson, Acta Mater. 51 (12) (2003) 3429–3443.
[13] D. Caillard, J.-.L. Martin, Thermally Activated Mechanisms in Crystal Plasticity, Elsevier, 2003.
[14] J.S. Harmon, M.D. Demetriou, W.L. Johnson, K. Samwer, Phys. Rev. Lett. 99 (2007), 135502.
[15] Z. Lu, J. W., W. W.H., B.H.Y, Phys. Rev. Lett. 113 (4) (2014), 045501.
[16] H.B. Yu, W.H. Wang, H.Y. Bai, K. Samwer, Natl. Sci. Rev. 1 (3) (2014) 429–461.
[17] K.L. Ngai, S. Capaccioli, Phys. Rev. E 69 (3) (2004), 031501.
[18] W. Dmowski, T. Iwashita, C.P. Chuang, J. Almer, T. Egami, Phys. Rev. Lett. 105 (20) (2010), 205502.
[19] J.C. Qiao, L.T. Zhang, Y. Tong, G.J. Lyu, Q. Hao, K. Tao, Advances in Mechanics in press doi: 10.6052/1000-0992-21-038 (2022).
[20] J.C. Ye, J. Lu, C.T. Liu, Q. Wang, Y. Yang, Nat. Mater. 9 (8) (2010) 619–623.
[21] H.-.B. Yu, M.-.H. Yang, Y. Sun, F. Zhang, J.-.B. Liu, C.Z. Wang, K.M. Ho, R. Richert, K. Samwer, J. Phys. Chem. Lett. 9 (19) (2018) 5877–5883.
[22] H.B. Yu, K. Samwer, Y. Wu, W.H. Wang, Phys. Rev. Lett. 109 (9) (2012), 095508.
[23] P.G. Debenedetti, F.H. Stillinger, Nature 410 (6825) (2001) 259–267.
[24] H.-.B. Yu, K. Samwer, Phys. Rev. B 90 (14) (2014), 144201.
[25] W. Johnson, K. Samwer, Phys. Rev. Lett. 95 (19) (2005), 195501.
[26] M. Bletry, P. Guyot, J.J. Blandin, J.L. Soubeyroux, Acta Mater. 54 (5) (2006) 1257–1263.
[27] Y. Shi, M.L. Falk, Phys. Rev. Lett. 95 (9) (2005), 095502.
[28] W. Dmowski, Y. Yokoyama, A. Chuang, Y. Ren, M. Umemoto, K. Tsuchiya, A. Inoue, T. Egami, Acta Mater. 58 (2) (2010) 429–438.
[29] F. Spaepen, Scr. Mater. 54 (3) (2006) 363–367.
[30] Y.-.J. Wang, M.Q. Jiang, Z.L. Tian, L.H. Dai, Scr. Mater. 112 (2016) 37–41.
[31] P. de Hey, J. Sietsma, A. van den Beukel, Acta Mater. 46 (16) (1998) 5873–5882.
[32] Y. Tong, W. Dmowski, H. Bei, Y. Yokoyama, T. Egami, Acta Mater. 148 (2018) 384–390.
[33] H.-.N. Lee, K. Paeng, S.F. Swallen, M.D. Ediger, Science 323 (5911) (2009) 231–234.
[34] P.Y. Huang, S. Kurasch, J.S. Alden, A. Shekhawat, A.A. Alemi, P.L. McEuen, J. P. Sethna, U. Kaiser, D.A. Muller, Science 342 (6155) (2013) 224–227.
[35] D. Han, D. Wei, P.-.H. Cao, Y.-.J. Wang, L.-.H. Dai, Phys. Rev. B 101 (6) (2020), 064205.
[36] M. Lüttich, V.M. Giordano, S.Le Floch, E. Pineda, F. Zontone, Y. Luo, K. Samwer, B. Ruta, Phys. Rev. Lett. 120 (13) (2018), 135504.
[37] B. Doliwa, A. Heuer, Phys. Rev. Lett. 91 (23) (2003), 235501.
[38] M. Yang, X.J. Liu, H.H. Ruan, Y. Wu, H. Wang, Z.P. Lu, J. Appl. Phys. 119 (24) (2016), 245112.
[39] J. Jiang, Z. Lu, J. Shen, T. Wada, H. Kato, M. Chen, Nat. Commun. 12 (1) (2021) 3843.
[40] Q. Zhou, Y. Du, W. Han, Y. Ren, H. Zhai, H. Wang, Scr. Mater. 164 (2019) 121–125.
[41] J. Kim, H.S. Oh, J. Kim, C.W. Ryu, G.W. Lee, H.J. Chang, E.S. Park, Acta Mater. 155 (2018) 350–361.